Acta Pharmaceutica Sinica B 2017;7(1):106–115

Chinese Pharmaceutical Association
Institute of Materia Medica, Chinese Academy of Medical Sciences

Acta Pharmaceutica Sinica B

www.elsevier.com/locate/apsb
www.sciencedirect.com

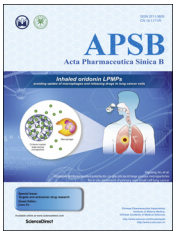

ORIGINAL ARTICLE

Synthesis of hydroxycinnamic acid derivatives as mitochondria-targeted antioxidants and cytotoxic agents

Jiyu Li[a,†], Dian He[a,†], Baitao Wang[a], Ling Zhang[a], Kun Li[a], Qinjian Xie[b], Lifang Zheng[a,*]

[a]*School of Pharmacy, Lanzhou University, Lanzhou 730000, China*
[b]*Gansu Corps Hospital of Chinese People Armed Police Forces, Lanzhou 730000, China*

Received 7 March 2016; received in revised form 20 April 2016; accepted 21 May 2016

KEY WORDS

Mitochondrial dysfunction;
Hepatocellular carcinomas;
Hydroxycinnamic acids;
Antiproliferative activities;
Mitochondrial permeability transition pore

Abstract In order to develop agents with superior chemopreventive and chemotherapeutic properties against hepatocellular carcinomas, mitochondria-targeted hydroxycinnamic acids (MitoHCAs) were synthesized by conjugation with a triphenylphosphonium cation. These synthetic compounds were evaluated for their antioxidant activities in hepatic mitochondria, including against $OH^{\bullet -}$ and $ROO^{\bullet -}$ induced lipid peroxidation. H_2O_2 production was decreased significantly by increasing glutathione peroxidase and catalase activities. In addition, cell proliferation data from three cell lines (HepG2, L02 and WI38) indicated that the MitoHCAs were selective for cancer cells. Interestingly, the MitoHCAs both with or without Ca^{2+} triggered mitochondrial dysfunction by inducing mitochondrial swelling, collapsing the mitochondrial membrane potential and causing cytochrome *c* release. In particular, an inhibitor of the mitochondrial permeability transition pore (mPTP), cyclosporin A, attenuated mitochondrial damage and cell apoptosis, indicating that mPTP may be involved in the antiproliferative activity of MitoHCAs. Further studies focused on structural optimization of these compounds are onging.

*Corresponding author. Tel./fax: +86 931 8915686.
E-mail address: zhenglf@lzu.edu.cn (Lifang Zheng).
†These authors made equal contributions to this work.
Peer review under responsibility of Institute of Materia Medica, Chinese Academy of Medical Sciences and Chinese Pharmaceutical Association.

http://dx.doi.org/10.1016/j.apsb.2016.05.002

1. Introduction

The liver is responsible for detoxifying noxious metabolites and requires substantial amounts of adenosine triphosphate (ATP) from mitochondria to fulfill this biological process. Prolonged exposure of the liver to detrimental xenobiotics causes oxidative damage to mitochondria[1,2]. The resulting defective mitochondria and decreased ATP synthesis may lead to the induction of hepatocellular carcinomas[3].

Hepatocellular carcinomas continue to be a major health concern and are ranked as the fifth most common cancer worldwide. In China, high incidence rates have accounted for 55% of the world's cases[4,5]. Typical treatments for hepatocellular carcinomas have included surgery, radiotherapy and chemotherapy, but current cure rates are not satisfactory[6]. Currently, mitochondria have been recognized as potential targets in cancer cells, as these organelles are a reservoir for proteins that promote apoptotic death when transported into the cytosol[7]. These findings underscore the importance of discovering mitochondria-targeted drugs that would protect healthy mitochondria from oxidative damage or selectively induce apoptosis in hepatocellular carcinomas, while simultaneously affecting as few healthy cells as possible.

Hence, mitochondria-targeted drugs have been developed using drug delivery carriers, such as the triphenylphosphonium (TPP) cation, mitochondria-targeted peptides, nanoparticles, cell penetrating peptides, etc[8]. The TPP cation allows for mitochondrial delivery *via* the electrical gradient across the mitochondrial inner membrane and has been developed by Murphy et al.[9]. Further, as a versatile therapeutic carrier, TPP-targeted drugs may exhibit selectivity towards tumor cells because cancer cells maintain a higher mitochondrial potential than non-malignant cells[10]. Additionally, because cancer mitochondria are structurally and functionally different from their normal counterparts, cancer cells display extensive metabolic reprogramming and are more susceptible to mitochondrial perturbations[7]. Therefore, mitochondria-targeted drugs have been synthesized based on active molecules, such as 1,4-naphthoquinone[11], resveratrol[12], coenzyme Q[13], etc.

In recent years natural products have generated significant interest as chemopreventive and chemotherapeutic agents[14,15]. Hydroxycinnamic acids (HCAs) and their derivatives are commonly isolated from Chinese medicinal herbs[16–18] and are found in some plant-derived food products[19]. Epidemiological studies have reported that coffee drinkers demonstrate a significant reduction in the risk for hepatocellular carcinomas when compared to non-drinkers[20]. Recently, caffeic acid was reported to protect rat liver from reperfusion injury *via* regulation of the *Sirt3*-mitochondrial respiratory chain pathway[21] and against *tert*-butyl hydroperoxide-induced oxidative hepatic damage[22]. Additionally, high doses of HCAs and their derivatives induced growth arrest and apoptosis in a variety of tumor cells by triggering either mitochondrial dysfunction or the mitochondria-dependent apoptotic pathway[23–25]. Despite the undoubted protective effects or anticancer efficacy, clinical trials have failed to establish a link between treatment with HCAs and cancer reduction, although this may be due to insufficient dosages to specific tissues[26,27].

In this study, mitochondria-targeted HCA derivatives (MitoHCAs) were synthesized (Scheme 1), where *p*-coumaric (*p*-CoA), caffeic (CaA), ferulic (FA) and cinnamic acid (CA) were conjugated to the TPP cation, consequently resulting in Mito*p*-CoA, MitoCaA, MitoFA and MitoCA, respectively. The synthesized MitoHCAs protected mitochondria from lipid peroxidation and decreased mitochondrial H_2O_2 levels by regulating antioxidant enzymes. In addition, they displayed high toxicity against human hepatoma HepG2 cells, but low toxicity toward two healthy cell lines—human hepatic L02 and diploid human fibroblasts WI38 cells. Further, MitoHCAs, both with and without Ca^{2+}, caused mitochondrial permeability transition pore (mPTP) opening, thereby collapsing the mitochondrial membrane potential (MMP) and causing cytochrome *c* (cyt *c*) release in isolated hepatic mitochondria, all of which initiate the apoptotic pathway[28]. Finally, cyclosporin A (CsA) attenuated MitoCaA-induced apoptosis and mitochondria damage.

2. Results and discussion

2.1. Synthesis

Synthesis of the MitoHCAs was performed as previously described (Scheme 1)[12,29]. The MitoHCAs were obtained in good yields (>70%) and were characterized by ^{1}H and ^{13}C NMR spectroscopy and HR-MS mass spectrometry (Supplementary Figs. S1–S4). The purity was >95%, as determined by HPLC analysis (Supplementary Fig. S5).

2.2. Inhibition of mitochondrial lipid peroxidation

As HCAs are excellent antioxidants, the synthesized MitoHCAs could act as novel inhibitors of mitochondrial lipid peroxidation. MitoCaA exhibited a dose-dependent suppression of lipid peroxidation causing full inhibition at ~6 μmol/L, while the parent compound CaA had no effect on lipid peroxidation induced by $FeCl_2$/ascorbate, which generates $OH^{\bullet}$ radicals *in situ*[30] (Fig. 1A). The inhibition potency of the synthesized MitoHCAs was measured: Mito*p*-CoA < MitoFA < MitoCaA (Fig. 1B). MitoCA and the control compounds (phosphonium salts butylTPP and CaA) were all ineffective at 6 μmol/L. Additionally, similar results were observed when mitochondria were treated with $ROO^{\bullet}$ radicals and MitoHCAs (Supplementary Fig. S3). Overall, these data suggest that the inhibitory potency of HCAs against mitochondrial lipid peroxidation was improved by addition of the TPP carrier.

2.3. Reduction of mitochondrial hydrogen peroxide levels and possible mechanisms

Supplementation with MitoHCAs protected liver mitochondrial lipids from exogenous ROS attack. In order to characterize this protection

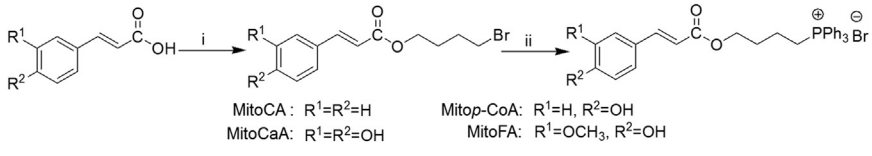

Scheme 1 Synthesis of MitoHCAs. Reagents and conditions: (i) $Br(CH_2)_4Br$, Et_3N, Me_2CO, 50 °C, 4 h (55%–65%); (ii) PPh_3, toluene, reflux, 36 h (70%–85%).

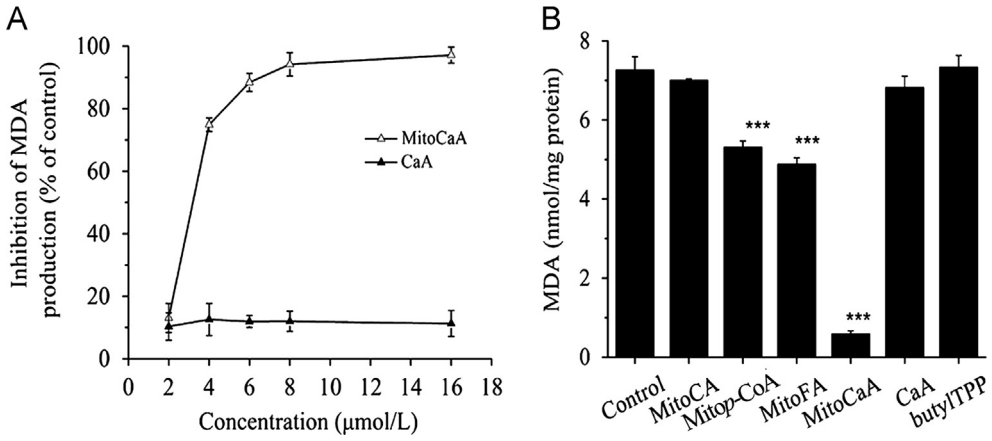

Figure 1 Inhibition of lipid peroxidation in the energized hepatic mitochondria (1 mg protein/mL) induced by $FeCl_2$/ascorbate supplementation. (A) In the presence of the various concentrations of MitoCaA and CaA. (B) In the presence of MitoHCAs, CaA and butylTPP (6 μmol/L). The values represent mean ± SEM of three independent experiments. $^{***}P<0.001$ *vs*. the control groups.

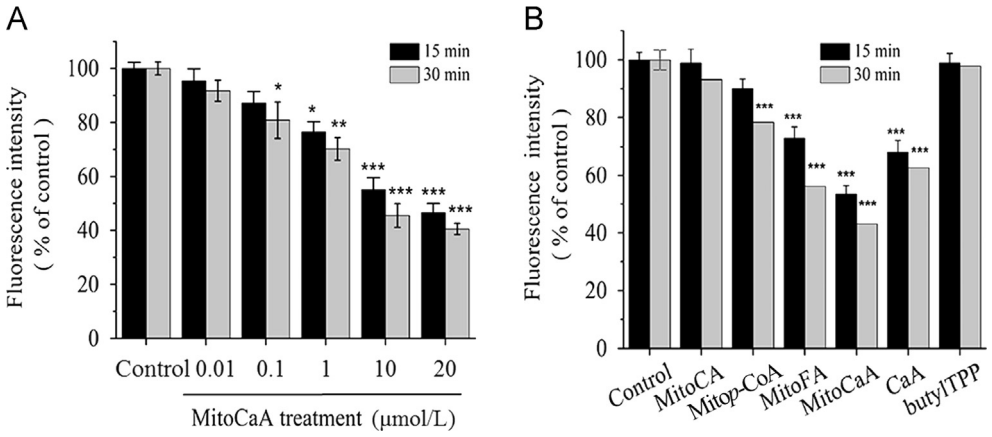

Figure 2 Inhibition of H_2O_2 production in energized hepatic mitochondria (1 mg protein/mL). (A) In the presence of the various concentrations of MitoCaA. (B) In the presence of MitoHCAs, CaA and butylTPP (10 μmol/L). The fluorescence of the DCFDA probe was monitored by excitation at 485 nm and recording the emission at 521 nm. The results were expressed as a percentage of the control. The values represent mean ± SEM of three independent experiments. $^{***}P<0.001$, $^{**}P<0.01$, $^{*}P<0.05$ *vs*. the control groups.

further, the effect of MitoHCAs on endogenous H_2O_2 generation in isolated hepatic mitochondria was investigated. H_2O_2 levels were measured by relative 2′,7′-di-chlorodihydrofluorescein diacetate (DCFDA) fluorescence. Incubation of mitochondria with MitoCaA significantly decreased H_2O_2 levels in both a concentration- and time-dependent manner (Fig. 2A). In order of increasing effect on H_2O_2 concentration was Mito*p*-CoA < CaA < MitoFA < MitoCaA. MitoCA and butylTPP did not affect the endogenous levels of H_2O_2 (Fig. 2B).

In order to further investigate the possible mechanisms by which MitoHCAs decreased mitochondrial H_2O_2 concentration, these compounds were assayed for their ability to directly scavenge H_2O_2, decrease $O_2^{-\bullet}$ production, or regulate antioxidant enzymes, for example, superoxide dismutase (SOD), glutathione peroxidase (GSH-Px) and catalase (CAT). No detectable changes in DCFDA fluorescence were noted after addition of MitoHCAs to H_2O_2, indicating that these compounds do not act as radical scavengers (results not shown). In addition, the MitoHCAs did not alter $O_2^{-\bullet}$ production in mitochondria as measured by dihydroethidium (DHE) probe fluorescence. Although MitoCA and butylTPP did not alter the activities of the antioxidant enzymes, MitoCaA, MitoFA and Mito*p*-CoA significantly increased both GSH-Px and CAT activities (Fig. 3). Interestingly, both Mito*p*-CoA and MitoCaA demonstrated ≤ 10% inhibition of mitochondrial SOD after 30 min, whereas MitoFA did not, which is consistent with previous observations that phenolic compounds do not inhibit SOD activity[31]. Together, these results suggest that MitoHCAs stimulate GSH-Px and CAT activites, thereby decreasing endogenous mitochondrial H_2O_2 levels.

2.4. *Antiproliferative activity*

Next, the antiproliferative activities of MitoHCAs against human hepatoma HepG2 cells and two normal cell lines, human hepatic L02 and diploid human WI38 fibroblasts, were investigated. With the knowledge that MitoHCAs target the mitochondria and would interfere with the MTT assay, the sulforhodamine B (SRB) method, which estimates cell number indirectly by measuring total protein content, was utilized instead, and this assay has

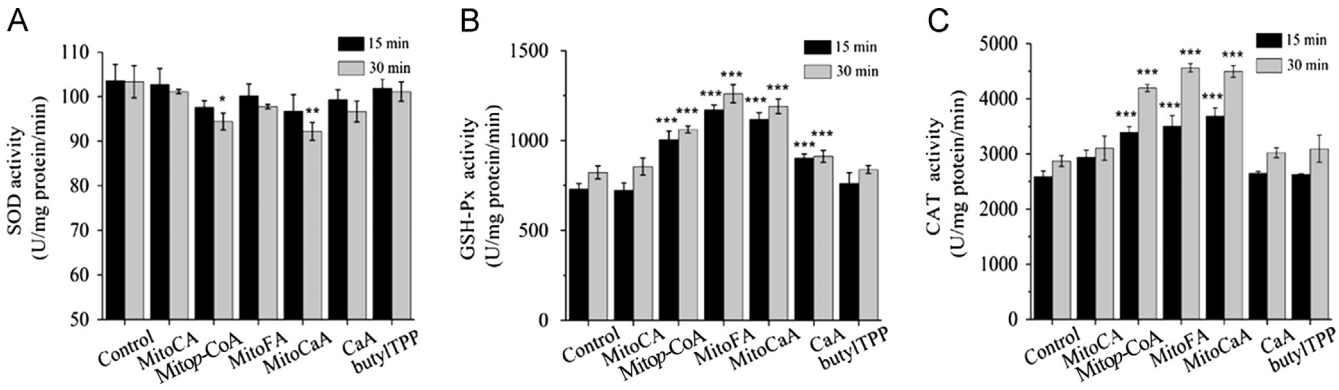

Figure 3 Impact of MitoHCAs on (A) SOD, (B) GSH-Px and (C) CAT activities. Energized hepatic mitochondria were incubated with the MitoHCAs (10 μmol/L) at 25 °C for 15 and 30 min. The enzyme assays were performed utilizing standardized kits. The values represent mean ± SEM of three independent experiments. $^{***}P<0.001$, $^{**}P<0.01$, $^{*}P<0.05$ *vs.* the control groups.

Table 1 Antiproliferative activity of MitoHCAs[a].

Compd.	IC_{50} (μmol/L)					
	HepG2		L02		WI38	
	24 h	48 h	24 h	48 h	24 h	48 h
MitoCA	11.22 ± 0.40	5.40 ± 0.32	105.42 ± 2.16	59.82 ± 5.77	126.50 ± 6.28	66.31 ± 2.16
Mito*p*-CoA	26.80 ± 1.53	15.33 ± 0.91	185.75 ± 6.39	80.57 ± 6.32	270.45 ± 8.05	112.57 ± 3.87
MitoFA	10.42 ± 0.37	6.49 ± 0.28	89.73 ± 3.47	50.72 ± 4.49	98.63 ± 2.18	53.52 ± 1.71
MitoCaA	9.19 ± 0.25	5.96 ± 0.21	118.68 ± 0.93	66.83 ± 3.49	123.57 ± 6.92	70.57 ± 2.15
CaA	200.89 ± 3.88	92.97 ± 1.35	402.95 ± 18.87	156.14 ± 8.83	280.89 ± 9.47	198.39 ± 7.78
ButylTPP	25.35 ± 1.02	12.81 ± 0.87	120.58 ± 9.97	71.42 ± 6.64	178.67 ± 3.73	88.51 ± 3.95

[a]Values represent mean ± SEM from at least three independent experiments.

Table 2 Therapeutic index (TI) of MitoHCAs.

Compd.	TI[a]	
	24 h	48 h
MitoCA	9.40	11.08
Mito*p*-CoA	6.93	5.26
MitoFA	8.61	7.82
MitoCaA	12.91	11.21
CaA	2.01	1.68
ButylTPP	4.76	5.58

[a]TI = IC_{50} L02 normal cell/IC_{50} HepG2 cancer cell.

proven to be the most suitable in the preclinical screening of novel therapeutic compounds[32]. In comparison to CA and butylTPP, MitoHCAs exhibited enhanced antiproliferative activities toward HepG2 cells (Table 1). MitoCA, MitoFA and MitoCaA were more toxic to the cells, resulting in IC_{50} values ~10 μmol/L at 24 h and ~6 μmol/L at 48 h. Moreover, MitoHCAs selectively inhibited proliferation in HepG2 cells in contrast to the non-cancerous L02 and WI38 cells; the IC_{50} values of the L02 and WI38 cells were 10-fold higher than for the HepG2 cells. The therapeutic index (TI) of MitoHCAs is calculated as the ratio of antiproliferative activities between normal cell and cancer cell lines (Table 2). The results revealed that the most active compound, MitoCaA, had the highest TI against HepG2 cells, with values of 12.91 at 24 h and 11.21 at 48 h, in comparison to compound CaA (TI = 2.01 and 1.68, respectively). This data indicates that the TPP-carrier molecule improved the antiproliferative activities of the synthesized HCAs, which is consistent with the mitochondria acting as a key organelle in controlling apoptosis.

2.5. *Induction of apoptosis and variations in mitochondrial morphology*

As MitoCaA displayed the optimal antiproliferative activities against HepG2 cells, the compound was further examined for its impact on cell apoptosis and mitochondrial morphology. Mito-Tracker Green FM was used to monitor mitochondrial morphology. MitoCaA triggered mitochondrial fragmentation after a 4-h treatment in a dose-dependent manner: treatment with 20 μmol/L MitoCaA resulted in donut-shaped morphology and a discontinuous network of mitochondria (Fig. 4A), in contrast to the filamentous or reticular mitochondria found in vehicle-treated cells. Noticeably, under the same experimental conditions, 20 μmol/L MitoCaA did not cause mitochondrial damage to normal L02 cells (Fig. 4A). Next, apoptotic cells were detected by AnnexinV–FITC/PI double staining. MitoCaA triggered apoptotic cell death in a dose-dependent manner (Fig. 4B). After treatment with 20 μmol/L MitoCaA for 24 h, FITC-positive cells accounted for 63.9% of the total cells, suggesting that apoptosis was a crucial pathway in the cytotoxicity of MitoCaA. This data

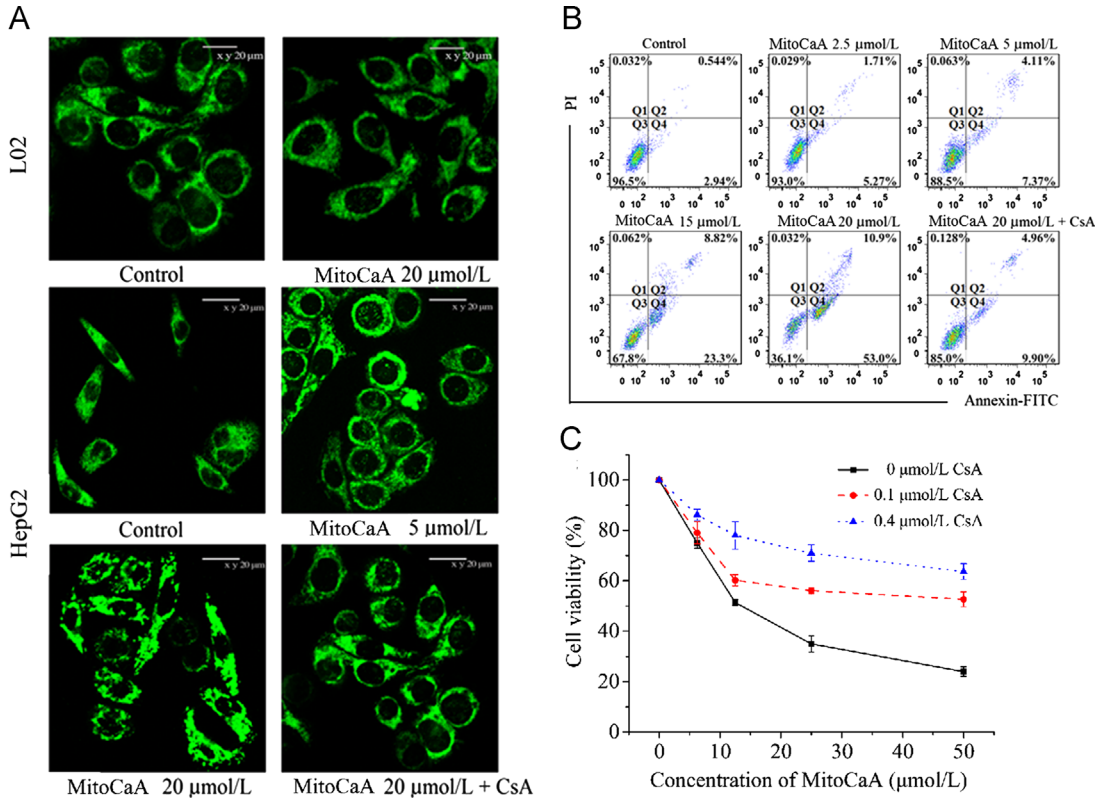

Figure 4 (A) Mitochondrial morphology of L02 cells and HepG2 cells treated with MitoCaA or MitoCaA+CsA (0.4 μmol/L) for 4 h. The mitochondrial network and morphology were visualized using MitoTracker Green FM staining and a confocal microscope. (B) Flow cytometry analyses for the apoptotic induction of HepG2 cells after 24 h treatment with MitoCaA or MitoCaA+CsA (0.4 μmol/L). (C) Cell viability of HepG2 cells after 24 h treatment with MitoCaA or MitoCaA+CsA. The values represent mean ± SEM of three independent experiments.

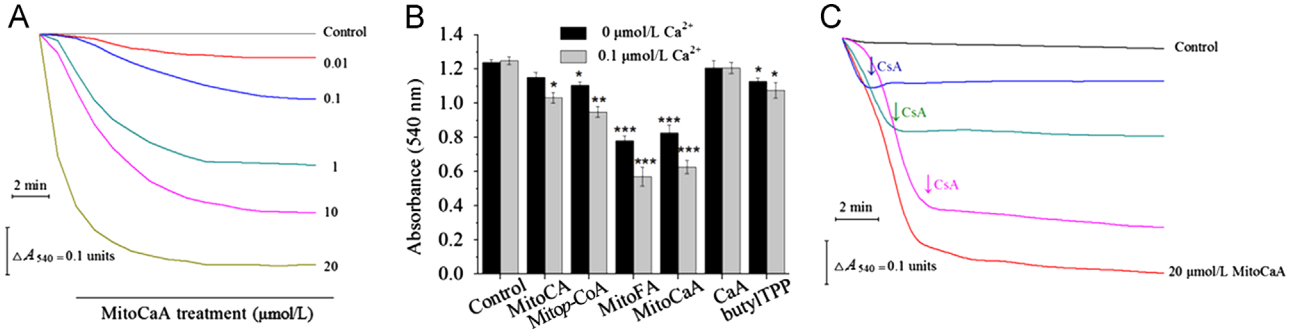

Figure 5 Detection of swelling in energized hepatic mitochondria (1 mg protein/mL). (A) In the presence of the various MitoCaA concentrations. (B) In the presence of 10 μmol/L MitoHCAs alone or 10 μmol/L MitoHCAs+Ca^{2+}. (C) Inhibition of 20 μmol/L MitoCaA-induced mitochondrial swelling by 1 μmol/L of CsA. CsA was added as indicated by the arrows. The assays were performed ≥ 4 times with similar results. The values represent mean ± SEM of three independent experiments. $^{***}P < 0.001$ *vs.* the control groups.

suggests that MitoCaA induced apoptotic cell death through mitochondrial impairment.

mPTP is known to be a critical component in drug-induced cell death. The opening of mPTP occurs in response to mitochondrial damage and the release of apoptotic factors, such as cyt *c*[28]. In order to determine if mPTP induction was involved in MitoCaA-induced apoptotic cell death, the effects of CsA, a known inhibitor of mPTP opening due to its interaction with cyclophilin D[28] on MitoCaA-induced cell death and mitochondrial morphology, were monitored. Interestingly, inclusion of CsA significantly attenuated cell death and mitochondrial damage in the MitoCaA model (Fig. 4). In sum, these results indicated mPTP involvement in MitoCaA-induced HepG2 cell death.

2.6. *Induction of mitochondrial dysfunction*

Based on the obtained results, the investigation was expanded to examine the impact of the compounds on the whole mitochondria. mPTP opening is often indicated by mitochondrial swelling. Isolated hepatic mitochondria were treated with MitoCaA (0.01–

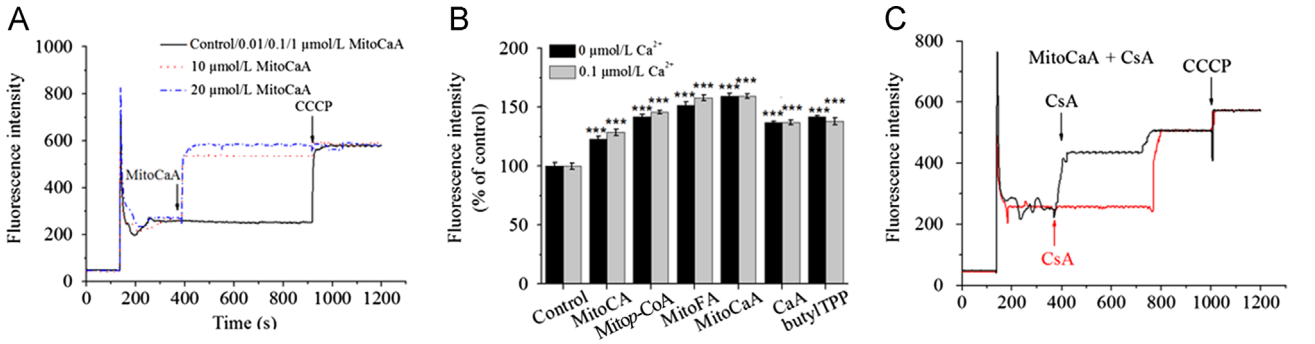

Figure 6 Collapse of mitochondrial membrane potential ($\Delta\Psi_m$). (A) In the presence of various MitoCaA concentrations. (B) In the presence of MitoHCAs, CaA and butylTPP (10 μmol/L) with and without Ca^{2+}. (C) In the presence of MitoCaA (10 μmol/L) with CsA (1 μmol/L). CsA was added as indicated by the arrows. The energized mitochondria suspensions (1 mg protein /mL) were incubated with 0.15 μmol/L of Rhodamine 123. 1 μmol/L CCCP, a respiratory uncoupler, was used to fully dissipate $\Delta\Psi_m$. The assays were performed $\geq$ 4 times with similar results. The values represent mean $\pm$ SEM of three independent experiments. $^{***}P<0.001$ *vs*. the control groups.

20 μmol/L) and an obvious decrease in absorbance was noted in a concentration-dependent manner, indicating large-amplitude swelling in the mitochondrial matrix (Fig. 5A). Next, the induction potency of various MitoHCAs was assessed, and neither MitoCA nor CaA induced swelling. The other compounds triggered swelling with increasing effect: butylTPP < Mito*p*-CoA < MitoFA $\approx$ MitoCaA (Fig. 5B). Ca^{2+} is a key stimulator involved in inducing the opening of the mPTP, and may trigger mPTP opening in combination with other stimuli[28]. During the resting state, the endogenous Ca^{2+} concentration should be $\sim$0.1 μmol/L in the mitochondria[33], but incubation with 0.1 μmol/L of Ca^{2+} had no effect on cell swelling under the tested conditions (Fig. 5B). However, treatment with MitoHCAs and Ca^{2+} intensified swelling, indicating that MitoHCAs had a synergistic interaction with Ca^{2+} to induce mPTP opening. Interestingly, the parent compound CaA failed to cause swelling, regardless of Ca^{2+} challenge, implying that CaA does not accumulate to high enough concentrations in the mitochondria matrix to induce swelling. In addition, swelling induced by MitoCaA was sensitive to CsA, as CsA blocked the swelling process immediately upon addition (Fig. 5C).

As mPTP opening may disrupt MMP, the effect of MitoHCAs on membrane potential was examined. Both 10 and 20 μmol/L MitoCaA promoted a transient decrease in MMP (Fig. 6A), with a decreasing affect among the synthesized compounds: MitoCA $\approx$ CaA $\approx$ butylTPP < Mito*p*-CoA < MitoFA < MitoCaA, roughly correlating with the previously noted induction of swelling (Fig. 6B). Treatment with CsA in MitoCaA-supplemented mitochondria delayed, but did not completely block, the dissipation of the MMP (Fig. 6C). In the presence of CsA, MMP was maintained for 400 s, after which the MMP level fully dissipated. 0.1 μmol/L Ca^{2+} was sufficient to diminish MMP in the presence of MitoHCAs, which was consistent with the synergistic induction of mPTP opening caused by Ca^{2+} (Fig. 6B).

The release of cyt *c* is a characteristic feature of the mitochondrial apoptotic pathway, which is downstream of mPTP opening[34]. After incubation with MitoHCAs, mitochondria released cyt *c*, as visualized by immunoblotting (Fig. 7A). However, in the presence of CsA, cyt *c* release was blocked (Fig. 7B). The total amount of cyt *c* was determined by dithionite-reduction assay, and MitoCaA induced the release of cyt *c* in a concentration-dependent manner (Fig. 7C). Incubation with 10 μmol/L of all MitoHCAs induced cyt *c* release (Fig. 7D). Both MitoFA and MitoCaA triggered significant release of 60 pmol cyt *c*/mg protein (about 2.5-fold *vs*. control). However, CaA and butylTPP had no effects. Synergistic release with Ca^{2+} was also observed (Fig. 7D). In summary, MitoFA and MitoCaA were able to trigger mitochondrial dysfunction. Ca^{2+}, as a key molecule in cell and mitochondria function, has synergistic actions with MitoHCAs in inducing mitochondrial damage. Further, CsA strongly prevented the mitochondrial dysfunction induced by MitoCaA.

3. Conclusions

Mitochondrial therapies, particularly those involving mitochondria-targeted antioxidants, have been considered to be effective in treating cancer[7,35]. In this study, a TPP carrier was used to target HCAs to mitochondria. The synthesized MitoHCAs improved the inherent biological activities of the parent compounds and the order of activities was MitoCA < Mito*p*-CoA < MitoFA $\approx$ MitoCaA, which was the similar to the biological activity order of parent compound HCAs[19]. MitoFA and MitoCaA have been identified as potent mitochondrial antioxidants and antiproliferative molecules with minimal toxicity toward non-cancerous cells. The protective effects of CsA suggested that mPTP was involved in cell death and mitochondrial dysfunction. The activity and mechanism of MitoFA and MitoCaA could guide further development of HCAs as potential therapeutic drugs against hepatocellular carcinomas.

4. Experimental section

4.1. *Materials and instruments*

All reagents and PRMI 1640 media were obtained from Sigma–Aldrich Ltd. (Beijing, China) or J&K Scientific Ltd. (Beijing, China). Antioxidant enzyme assay kits were purchased from Nanjing Jiancheng Bioengineering Institute (Nanjing, China). The BCA protein assay kit was obtained from Beyotime Institute of Biotechnology (Jiangsu, China). Polyvinylidine fluoride membranes and Centricon YM-3 were purchased from the Millipore Corp. (USA). Rabbit anti-cyt *c* (AF0146) and rabbit anti-VDAC1 (DF6140) were obtained from Affinity Biosciences (OH, USA).

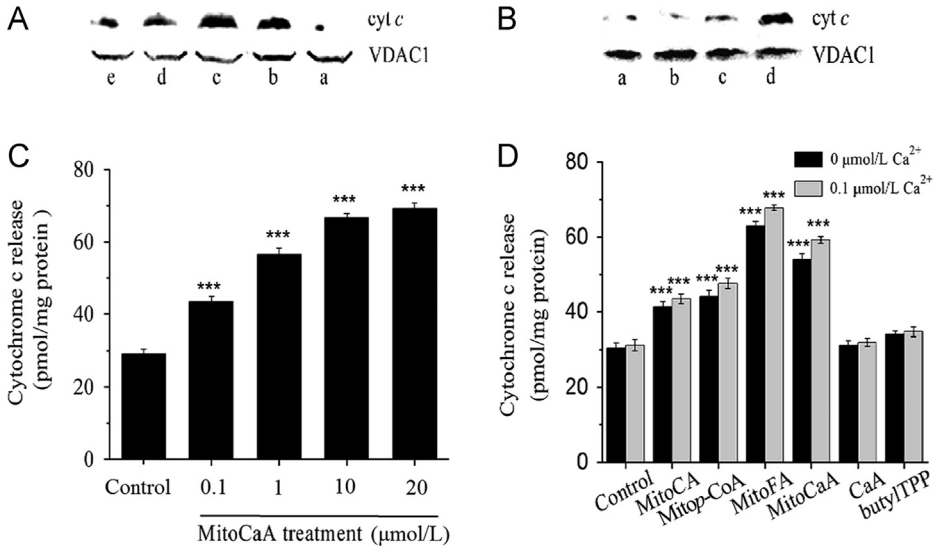

Figure 7 Detection of cyt *c* release from energized mitochondria suspensions (2 mg protein/mL). (A) In the presence of 10 μmol/L MitoHCAs. a: control; b: MitoCaA; c: MitoFA; d: Mito*p*-CoA; e: MitoCA. (B) a: control; b: 1 μmol/L MitoCaA; c: 20 μmol/L MitoCaA +1 μmol/L CsA; d: 20 μmol/L MitoCaA. The blots shown are representative of three independent experiments demonstrating similar results. (C) In the presence of the various concentrations of MitoCaA. (D) In the presence of MitoHCAs, CaA and butylTPP (10 μmol/L) with or without Ca^{2+}. The quantitative assays were performed by the dithionite-reduction method. The values represent mean ± SEM of three independent experiments. $^{***}P<0.001$ *vs.* the control groups.

Fetal bovine serum was purchased from Hangzhou Sijiqing Biomaterials Co., Ltd. (Hangzhou, China).

^{1}H NMR and ^{13}C NMR spectra were recorded using a Varian Mercury spectrometer operating at 400 MHz for ^{1}H NMR and 100 MHz for ^{13}C NMR. HR-MS spectra were obtained on an Orbitrap Elite (Thermo Scientific) mass spectrometer. UV/Vis spectra were recorded at 25 °C with a Perkin-Elmer Lambda 25 spectrophotometer that was equipped with temperature-controlled cell holders (USA). Fluorescence intensity and fluorescence spectra were measured at 25 °C with an Infinite M200 Pro Multimode Reader (Switzerland) and a Shimadzu RF-5301 spectrofluorimeter (Japan), respectively.

4.2. *Chemistry*

4.2.1. *Synthesis procedures*

The MitoHCAs and intermediates were synthesized according to previously reported procedures[12,29]. The chemical structures were confirmed by ^{1}H and ^{13}C NMR, HR-MS-ESI (Supplementary Figs. S1–S4)

(E)-4-(3-Phenyl)acrylate butyltriphenylphosphonium bromate (MitoCA): 85% yield; ^{1}H NMR (400 MHz, DMSO-d_6): δ: 1.68 (m, 2H, CH_2), 1.86 (m, 2H, CH_2), 3.71 (m, 2H, CH_2-P), 4.21 (m, 2H, OCH_2), 6.54 (d, 1H, J=16Hz, H-α), 7.44–7.46 (m, 3H, H-3, H-4, H-5), 7.58 (d, 1H, J=16 Hz, H-β), 7.76–7.79 (m, 2H, H-2, H-6), 7.81–7.89 (m, 15H, PPh_3); ^{13}C NMR (100 MHz, DMSO-d_6): δ: 18.93, 20.02, 29.15, 63.27, 118.35, 118.48, 119.33, 128.80, 130.65, 131.03, 134.02, 134.37, 135.35, 144.99, 166.56; HR-MS: Calcd. for $C_{31}H_{30}O_2P$, 465.1978; found 465.1970, error 1.7 ppm.

(E)-4-(3-(4-Hydroxyphenyl) acrylate butyltriphenylphosphonium bromate) (Mitop-CoA): 75% yield; ^{1}H NMR (400 MHz, DMSO-d_6): δ: 1.66 (m, 2H, CH_2), 1.82 (m, 2H, CH_2), 3.65 (m, 2H, CH_2-P), 4.17 (m, 2H, OCH_2), 6.28 (d, 1H, J=16 Hz, H-α), 6.80 (d, 2H, J=8.8 Hz, H-3, H-5), 7.51 (d, 1H, J=16 Hz, H-β), 7.53 (d, 2H, J=8.8 Hz, H-2, H-6), 7.73–7.90 (m, 15H, PPh_3), 10.05 (s, 1H, OH); ^{13}C NMR (100 MHz, DMSO-d_6): δ: 19.81, 19.63, 28.87, 62.59, 114.10, 115.87, 118.13, 125.13, 130.31, 133.67, 135.02, 144.87, 159.87, 166.61; HR-MS: Calcd. for $C_{31}H_{30}O_3P$, 481.1927; found 481.1919, error 1.7 ppm.

(E)-4-(3-(4-Methoxyphenyl) acrylate butyltriphenylphosphonium bromate) (MitoFA): 70% yield; ^{1}H NMR (400 MHz, $CDCl_3$): δ: 1.72 (m, 2H, CH_2), 2.16 (m, 2H, CH_2), 3.93 (s, 3H, -OCH_3), 4.01 (m, 2H, CH_2-P), 4.23 (m, 2H, OCH_2), 6.15 (d, 1H, J=15.6 Hz, H-α), 6.99–7.05 (m, 3H, H-2, H-5, H-6), 7.52 (d, 1H, J=15.6 Hz, H-β), 7.65–7.89 (m, 15H, PPh_3); ^{13}C NMR (100 MHz, $CDCl_3$): δ: 19.17, 21.84, 29.01, 56.04, 62.82, 109.77, 114.77, 115.02, 117.69, 122.82, 126.51, 130.36, 133.54, 134.94, 145.12, 147.03, 148.42, 167.20; HR-MS: Calcd. for $C_{32}H_{32}O_4P$, 511.2033; found 511.2088, error 1.0 ppm.

(E)-4-(3-(3,4-Dihydroxyphenyl) acrylate butyltriphenylphosphonium bromate) (MitoCaA): 81% yield; ^{1}H NMR (400 MHz, DMSO-d_6): δ: 1.63 (m, 2H, CH_2), 1.81 (m, 2H, CH_2), 3.66 (m, 2H, CH_2-P), 4.14 (m, 2H, OCH_2), 6.13 (d, 1H, J=16 Hz, H-α), 6.76 (d, 1H, J=8 Hz, H-5), 6.94 (d, 1H, J=8 Hz, H-6), 7.03 (s, 1H, H-2), 7.37 (d, 1H, J=15.6 Hz, H-β), 7.76–7.86 (m, 15H, PPh_3), 9.19 (s, 1H, OH), 9.66 (s, 1H, OH); ^{13}C NMR (100 MHz, DMSO-d_6): δ: 18.55, 19.60, 28.84, 62.53, 113.84, 114.86, 115.87, 118.12, 121.53, 125.50, 130.29, 133.66, 135.00, 145.25, 145.70, 148.58, 166.54; HR-MS: Calcd. for $C_{31}H_{30}O_4P$, 497.1876; found 497.1880, error 0.8 ppm.

4.2.2. *HPLC purity analysis*

HPLC analysis was performed using a Waters 600 system equipped with a Waters 2998 photodiode array detector, including a 2707 automatic injector and a computer integrating apparatus. The column was a Diamonsil C18 (150 mm × 4.6 mm, 5 μm) and the column compartment was kept constant at 25 °C. The injection volume was 20.0 μL. Two mobile phases were used: (1) methanol: acetate buffer (50:50, *v*/*v*, pH=3.2), flow-rate of 1 mL/min. (2) acetonitrile:acetate buffer (50:50, *v*/*v*, pH=4.0), flow-rate of

0.5 mL/min. Detection was measured at 300 nm. The results and spectra are shown in Supplementary Fig. S2.

4.3. Biological studies

For the subsequent assays, the MitoHCAs were dissolved in DMSO, with the final concentrations of each reactant indicated in parentheses. The final DMSO concentration did not exceed 0.1% (*v/v*) and did not affect the results from the assays.

4.3.1. Preparation of hepatic mitochondria

Male Wister rats weighting 250 ± 20 g, obtained from the animal center of the Medical College of Lanzhou University, were fasted overnight before cervical dislocation. All the animals were cared for and experiments were carried out in accordance with the principles and guidelines of the National Institutes of Health guide for the care and use of laboratory animals. All the protocols were approved by the Ethics Committee of Lanzhou University. Mitochondria were isolated by a standard differential centrifugation protocol[36]. The protein concentration was determined by biuret assay, using BSA as a standard[37]. For subsequent assays mitochondrial suspensions were incubated in the standard medium (in mmol/L: sucrose 250, HEPES 10, KH_2PO 1, glutamate 10, malate 5; pH 7.4).

4.3.2. Mitochondrial lipid peroxidation assay

In order to quantify the amount of lipid peroxidation in mitochondria suspended in the standard medium (1 mg/mL), the TBARS assay was used[38]. The final concentrations of reactants are indicated in parentheses. The peroxidation reaction was initiated by addition of $FeCl_2$ (20 μmol/L)/ascorbate (100 μmol/L) or AAPH (10 mmol/L), and inhibited by addition of the MitoHCAs (6 μmol/L). After incubation for 30 min, a TCA-TBA-HCl stock solution (15% *w/v* TCA; 0.375% *w/v* TBA; 0.25 mol/L HCl), together with 0.02% (*w/v*) butylated hydroxytoluene, was added. The solution was heated in a hot-water bath for 15 min. After cooling to room temperature, the precipitate was removed by centrifugation and the absorbance of the supernatant was determined at 532 nm[38]. The amount of malondialdehyde (MDA) was calculated using $\varepsilon_{532} = 1.5 \times 10^5$ mol/(L · cm).

4.3.3. Measurement of mitochondrial H_2O_2 and $O_2^{-\bullet}$ production

H_2O_2 and $O_2^{-\bullet}$ production were assessed using the fluorescents probes DCFDA and DHE, respectively[39]. DCFDA probe (8 μmol/L) or DHE probe (5 μmol/L) was added to 1 mg/mL of energized mitochondria suspension in the standard medium. MitoHCAs were added and the suspension was incubated for either 15 or 30 min in the dark at 25 °C. DCFDA was detected with excitation and emission wavelengths of 485 nm and 521 nm, respectively. DHE was detected with excitation and emission wavelengths of 470 nm and 585 nm, respectively.

4.3.4. Measurement of mitochondrial SOD, GPx and CAT activities

Mitochondrial SOD, GSH-Px and CAT activities were determined according to the instructions from the commercial kits (Nanjing Jiancheng Bioengineering Institute). Briefly, after incubation with the tested compounds for 15 or 30 min at 30 °C, the mitochondria were sonicated at 400 A every 5 s for 5 cycles. Enzyme activities were determined as described in the instructions. Controlled experiments determined that the tested compounds did not interfere with the assays.

4.3.5. Cell culture

HepG2, L02, and WI38 cells were obtained from the Shanghai Institute of Biochemistry and Cell Biology, Chinese Academy of Science. HepG2 cells were cultured in 1640 media supplemented with 10% fetal bovine serum and 1% penicillin-streptomycin at 37 °C under a 5% CO_2 atmosphere. L02 and WI38 cells were cultured in DMEM media supplemented with 10% fetal bovine serum and 1% penicillin–streptomycin at 37 °C under a 5% CO_2 atmosphere.

4.3.6. SRB assay

Antiproliferative activity was determined using the SRB assay, which estimates cell number indirectly by measuring total protein concentration. 5×10^4 adherent cells/well were incubated in 96-well microtiter plates for 24 h. Following the addition of the test compounds the plates were incubated for an additional 24 h and 48 h, after which the plates were treated as described by the standard SRB method[32]. The absorbance was read at 540 nm on a microplate reader. IC_{50} values were determined from a log plot of percent of control *versus* concentration.

4.3.7. Flow cytometric analysis

HepG2 cells (5×10^5/well) were seeded in six-well plates and incubated for 24 h to allow for exponential growth and then treated with the test compounds for another 24 h. The cells were collected and washed with phosphate-buffered saline (PBS). Apoptotic cells were labeled with annexinV–FITC/PI according to the manufacturer's instructions (Beyotime Institute of Biotechnology, Jiangsu, China). Cells were analyzed on a FACSCanto flow cytometer (Becton Dickinson, LSRFortessa, USA).

4.3.8. Measurement of mitochondrial morphology

HepG2 cells were grown on coverslips at 5×10^5 cells/wells inside 6-well plates overnight and then treated with the test compounds for 4 h. After treatment, the media was removed from the dish and the cells were washed 3 times with pre-warmed PBS. The cells were stained and incubated at 37 °C for 30 min with 50 nmol/L MitoTracker Green FM. After staining, cells were washed twice with PBS. The coverslips were inverted onto glass slides with 10 μL of an antifade mounting medium (Beyotime). Confocal images were obtained using a confocal laser-scanning microscope (Zessi, LSM 510 META, Germany).

4.3.9. Measurement of mitochondrial membrane potential and swelling

MMP was measured using the fluorescence dye Rhodamine 123[40]. Briefly, 0.15 μmol/L Rhodamine 123 was added to energized isolated hepatic mitochondria (1 mg/mL) in the standard medium (excitation and emission wavelengths of 503 and 523 nm, respectively). After a short incubation for signal stabilization, the compounds were added as indicated in the legend to Fig. 6. Finally, the respiratory uncoupler CCCP (1 μmol/L) was used to fully depolarize MMP. Mitochondrial swelling was determined by measuring the apparent A_{540} change of the mitochondrial suspension[41]. Energized isolated hepatic mitochondria (1 mg/mL) were incubated in the standard medium. Further compounds were added as indicated in the Fig. 5 legend.

4.3.10. Measurement of cyt c release

Immunoblotting was performed as follows: the mitochondria (2 mg protein/mL) were incubated for 15 min at 25 °C in standard

medium with the test compounds. The reaction mixtures were then centrifuged at 12,000 × *g* for 10 min at 4 °C to obtain mitochondrial pellets. The supernatant fractions were centrifuged further at 100,000 × *g* for 15 min at 4 °C to eliminate mitochondrial membrane fragments, and then were concentrated by ultrafiltration with a Centricon YM-3. Twenty microliter aliquots of the concentrated supernatants were subjected to electrophoresis on a 12% SDS-PAGE gel. The gel was transferred to a polyvinylidine fluoride membrane for immunoblotting analysis. VDAC1 was used as a loading control. The protein bands were visualized using the Gel Imaging System (ChemDoc-It610, UVP, USA). The dithionite-reduction assay was performed as follows: (1) energized hepatic mitochondria (2 mg/mL) were treated with MitoHCAs at the desired concentrations for 15 min; (2) mitochondria were centrifuged at 12,000 × *g* for 10 min; (3) dithionite (1.2 mg) was added to 4.0 mL of the supernatant; (4) the amount of cyt *c* was determined at 550 nm[42]. The extinction coefficient of $E^{1\%}_{1\ cm}$ is 23.

4.3.11. *Statistical analysis*

The data are expressed as the mean ± SEM. Statistical differences between two groups were assessed by the Student's *t*-test. And $P < 0.05$ was used as the criterion for statistical significance.

Acknowledgments

This work was supported by the National Natural Sciences Foundation of China (Grant No. 21302079), and the Fundamental Research Funds for the Central Universities (No. lzujbky2014151).

Appendix A. Supporting information

Supplementary data associated with this article can be found in the online version at http://dx.doi.org/10.1016/j.apsb.2016.05.002.

References

1. Choi J, Corder NLB, Koduru B, Wang YY. Oxidative stress and hepatic Nox proteins in chronic hepatitis C and hepatocellular carcinoma. *Free Radic Biol Med* 2014;**72**:267–84.
2. Cardin R, Piciocchi M, Bortolami M, Kotsafti A, Barzon L, Lavezzo E, et al. Oxidative damage in the progression of chronic liver disease to hepatocellular carcinoma: an intricate pathway. *World J Gastroenterol* 2014;**20**:3078–86.
3. Auger C, Alhasawi A, Contavadoo M, Appanna VD. Dysfunctional mitochondrial bioenergetics and the pathogenesis of hepatic disorders. *Front Cell Dev Biol* 2015;**3**:40.
4. Fang JY, Wu KS, Zeng Y, Tang WR, Du PL, Xu ZX, et al. Liver cancer mortality characteristics and trends in China from 1991 to 2012. *Asian Pac J Cancer Prev* 2015;**16**:1959–64.
5. Zuo TT, Zheng RS, Zhang SW, Zeng HM, Chen WQ. Incidence and mortality of liver cancer in China in 2011. *Chin J Cancer* 2015;**34**:508–13.
6. Chiu CC, Wang JJ, Chen YS, Chen JJ, Tsai TC, Lai CC, et al. Trends and predictors of outcomes after surgery for hepatocellular carcinoma: a nationwide population-based study in Taiwan. *Eur J Surg Oncol* 2015;**41**:1170–8.
7. Weinberg SE, Chandel NS. Targeting mitochondria metabolism for cancer therapy. *Nat Chem Biol* 2015;**11**:9–15.
8. Han M, Li C, Guo WW, Liu HN, Liang WQ, Gao JQ. Mitochondrial drug delivery for cancer therapy. *Acta Pharm Sin* 2016;**51**:257–63.
9. Murphy MP, Smith RA. Targeting antioxidants to mitochondria by conjugation to lipophilic cations. *Annu Rev Pharmacol Toxicol* 2007;**47**:629–56.
10. Modica-Napolitano JS, Aprille JR. Delocalized lipophilic cations selectively target the mitochondria of carcinoma cells. *Adv Drug Deliv Rev* 2001;**49**:63–70.
11. Lu X, Altharawi A, Gut J, Rosenthal PJ, Long TE. 1,4-Naphthoquinone cations as antiplasmodial agents: hydroxy-, acyloxy-, and alkoxy-substituted analogues. *ACS Med Chem Lett* 2012;**3**:1029–33.
12. Biasutto L, Mattarei A, Marotta E, Bradaschia A, Sassi N, Garbisa S, et al. Development of mitochondria-targeted derivatives of resveratrol. *Bioorg Med Chem Lett* 2008;**18**:5594–7.
13. Jin H, Kanthasamy A, Ghosh A, Anantharam V, Kalyanaraman B, Kanthasamy AG. Mitochondria-targeted antioxidants for treatment of Parkinson's disease: preclinical and clinical outcomes. *Biochim Biophys Acta* 2014;**1842**:1282–94.
14. Kumar H, Kim IS, More SV, Kim BW, Choi DK. Natural product-derived pharmacological modulators of Nrf2/ARE pathway for chronic diseases. *Nat Prod Rep* 2014;**31**:109–39.
15. Butler MS, Robertson AA, Cooper MA. Natural product and natural product derived drugs in clinical trials. *Nat Prod Rep* 2014;**31**:1612–61.
16. Jiang RW, Lau KM, Hon PM, Mak TCW, Woo KS, Fung KP. Chemistry and biological activities of caffeic acid derivatives from *Salvia miltiorrhiza*. *Curr Med Chem* 2005;**12**:237–46.
17. Yi LZ, Liang YZ, Wu H, Yuan DL. The analysis of Radix Angelicae Sinensis (Danggui). *J Chromatogr A* 2009;**1216**:1991–2001.
18. Li F, Cao QE, Ding ZT. Separation and determination of three phenylpropanoids in the traditional Chinese medicine and its preparations by capillary electrophoresis. *J Chromatogr Sci* 2007;**45**:354–9.
19. El-Seedi HR, El-Said AM, Khalifa SA, Göransson U, Bohlin L, Borg-Karlson AK, et al. Biosynthesis, natural sources, dietary intake, pharmacokinetic properties, and biological activities of hydroxycinnamic acids. *J Agric Food Chem* 2012;**60**:10877–95.
20. Nkondjock A. Coffee consumption and the risk of cancer: an overview. *Cancer Lett* 2009;**277**:121–5.
21. Mu HN, Li Q, Pan CS, Liu YY, Yan L, Hu BH, et al. Caffeic acid attenuates rat liver reperfusion injury through sirtuin 3-dependent regulation of mitochondrial respiratory chain. *Free Radic Biol Med* 2015;**85**:237–49.
22. Yang SY, Hong CO, Lee GP, Kim CT, Lee KW. The hepatoprotection of caffeic acid and rosmarinic acid, major compounds of *Perilla frutescens*, against *t*-BHP-induced oxidative liver damage. *Food Chem Toxicol* 2013;**55**:92–9.
23. Chang WC, Hsieh CH, Hsiao MW, Lin WC, Hung YC, Ye JC. Caffeic acid induces apoptosis in human cervical cancer cells through the mitochondrial pathway. *Taiwan J Obstet Gynecol* 2010;**49**:419–24.
24. Shailasree S, Venkataramana M, Niranjana SR, Prakash HS. Cytotoxic effect of *p*-coumaric acid on neuroblastoma, N2a cell *via* generation of reactive oxygen species leading to dysfunction of mitochondria inducing apoptosis and autophagy. *Mol Neurobiol* 2015;**51**:119–30.
25. Hemaiswarya S, Doble M. Combination of phenylpropanoids with 5-fluorouracil as anti-cancer agents against human cervical cancer (HeLa) cell line. *Phytomedicine* 2013;**20**:151–8.
26. Mancuso C, Santangelo R. Ferulic acid: pharmacological and toxicological aspects. *Food Chem Toxicol* 2014;**65**:185–95.
27. Saso L, Firuzi O. Pharmacological applications of antioxidants: lights and shadows. *Current Drug Targets* 2014;**15**:1177–99.
28. Dalla Via L, García-Argáez AN, Martínez-Vázquez M, Grancara S, Martinis P, Toninello A. Mitochondrial permeability transition as target of anticancer drugs. *Curr Pharm Des* 2014;**20**:223–44.
29. Chen L, Zhang YH, Kong XW, Peng SX, Tian JD. Synthesis and biological evaluation of nitric oxide-releasing derivatives of oleanolic acid as inhibitors of HepG2 cell apoptosis. *Bioorg Med Chem Lett* 2007;**17**:2979–82.
30. Wills ED. Lipid peroxide formation in microsomes. General considerations. *Biochem J* 1969;**113**:315–24.

31. Lagoa R, Graziani I, Lopez-Sanchez C, Garcia-Martinez V, Gutierrez-Merino C. Complex I and cytochrome *c* are molecular targets of flavonoids that inhibit hydrogen peroxide production by mitochondria. *Biochim Biophys Acta* 2011;**1807**:1562–72.
32. van Tonder A, Joubert AM, Cromarty AD. Limitations of the 3-(4,5-dimethylthiazol-2-yl)-2,5-diphenyl-2*H*-tetrazolium bromide (MTT) assay when compared to three commonly used cell enumeration assays. *BMC Res Notes* 2015;**8**:47.
33. Lu JW, Zhai YJ, Sun F. Research of mitochondrial calcium transportation. *Acta Biophys Sin* 2013;**29**:167–80.
34. Yang JC, Cortopassi GA. Induction of the mitochondrial permeability transition causes release of the apoptogenic factor cytochrome *c*. *Free Radic Biol Med* 1998;**24**:624–31.
35. Olszewska A, Szewczyk A. Mitochondria as a pharmacological target: magnum overview. *IUBMB Life* 2013;**65**:273–81.
36. Zhao YB, Ye LH, Liu HX, Xia Q, Zhang Y, Yang XD, et al. Vanadium compounds induced mitochondria permeability transition pore (PTP) opening related to oxidative stress. *J Inorg Biochem* 2010;**104**:371–8.
37. Gornall AG, Bardawill CJ, David MM. Determination of serum proteins by means of the biuret reaction. *J Biol Chem* 1949;**177**:751–66.
38. Buege JA, Aust SD. Microsomal lipid peroxidation. *Methods Enzymol* 1978;**52**:302–10.
39. Degli Esposti M. Measuring mitochondrial reactive oxygen species. *Methods* 2002;**26**:335–40.
40. Scaduto Jr. RC, Grotyohann LW. Measurement of mitochondrial membrane potential using fluorescent rhodamine derivatives. *Biophys J* 1999;**76**:469–77.
41. Petronilli V, Cola C, Massari S, Colonna R, Bernardi P. Physiological effectors modify voltage sensing by the cyclosporin A–sensitive permeability transition pore of mitochondria. *J Biol Chem* 1993;**268**:21939–45.
42. The State Pharmacopoeia Committee of China. *Pharmacopoeia of the People's Republic of China.* vol. II. Beijing: China Medical and Technology Press; 2015.